Supporting Information

Insight the Zn^{2+} storage mechanism in V_6O_{13} with Nano-sheets for High-capacity and Long-life Aqueous Zinc-Metal Batteries

Lineng Chen[a], Wenwei Zhang[a], Jianyong Zhang[a], Qinyou An[a,b,*]

a. State Key Laboratory of Advanced Technology for Materials Synthesis and Processing, Wuhan University of Technology, Wuhan 430070, China

b. Hubei Longzhong Laboratory, Wuhan University of Technology (Xiangyang Demonstration Zone), Xiangyang, 441000, P. R. China

Experimental section

Materials synthesis

The V_6O_{13} nanosheets were prepared in two steps. Firstly, 0.85 g ammonium metavanadate and 1.06 g oxalic acid dihydrate (ratio mass 1:0.9) were dispersed into 30 mL deionized water, after 1 h magnetic force stirring, the yellow-green transparent solution was obtained. Subsequently, the mixture was transferred to a 50 mL Teflon-lined autoclave to be maintained at 180 °C for 48 h. After washed with deionized water and ethanol for several times, flowerlike $NH_4V_4O_{10}$ precursor were finally collected by dried at 80°C overnight. Secondly, V_6O_{13} nanosheet was obtained by annealing the precursor at 450 ℃ for 8 h in H_2/Ar (5/95) atmosphere at heating rate of 5℃ min^{-1}. In this process, NH_3 decomposed from $NH_4V_4O_{10}$ acts as a reducing agent to facilitate the production of mixed valence vanadium with high electrical conductivity.

Material characterizations

The crystallographic characterization of the product was measured by a Bruker D8 Advance X-ray diffractometer with Cu-Kα radiation (λ=1.5418 Å). Field emission scanning electron microcopy (FESEM) images were obtained with a JEOL-7100F microscope. Energy dispersive X-ray spectra (EDS) was recorded using an Oxford EDS IE250 system. Transmission electron microscopy (TEM) and high-

resolution transmission electron microscopy (HRTEM) images were collected with a Thermo Fisher Scientific Talos F200S microscope. Raman spectrum measurement was achieved using a Renishaw RM-1000 laser Raman microscopy system. X-ray photoelectron spectroscopy (XPS) measurements were performed using a VG Multi Lab 2000 instrument. XPS measurement was performed with a VG Multi Lab 2000 instrument. The X-ray absorption near-edge structure (XANES) and Fourier transform extended X-ray absorption fine structure (FT-EXAFS) extended X-ray absorption spectroscopy data reduction and analysis followed standard methods using the ATHENA software package.

Electrochemical measurements

To conduct the electrochemical measurements, the AZIBs were assembled with CR2016-type coin cells in the air atmosphere. The working electrodes was prepared by mixing 60 % V_6O_{13} nanosheets, 30 % acetylene black, and 10 % poly tetrafluoroethylene (PTFE), the solvents is isopropyl alcohol which is volatile, then the slurry was evenly grinded, tableted and cut into cut into small wafers with a diameter of Φ6 mm, the mass loading is about 1.42 mg cm^{-2}. Zinc foil and 1 mol L^{-1} $Zn(CF_3SO_3)_2$ solution were used as the anode and electrolyte, respectively, and GF/A glass fiber membrane from What-man was used as the separator. The galvanostatic discharge-charge tests were performed with a battery test system (LAND CT2001A). Cyclic voltammograms (CV) and EIS were carried out on a multi-channel electrochemical workstation (VMP3 Bio-Logic France). For the in-situ characterization, the beryllium window used in traditional in-situ testing would react with electrolyte in AZIBs system, so an improved in-situ monitoring device was employed. The new cathode shell had a Φ2 mm circular hole served as an information collection window for in-situ monitoring. The cell was cycled at a current density of 500 mA g^{-1}.

Supplementary Figures

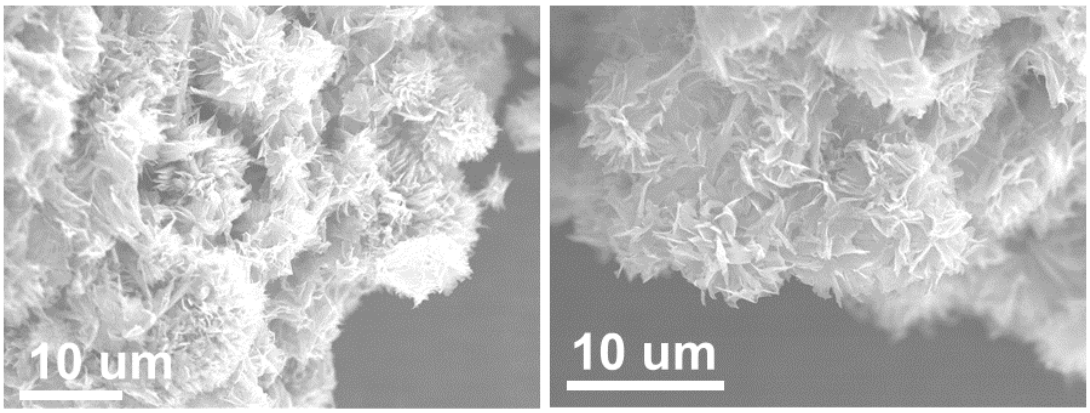

Figure S1. SEM image of precursor $NH_4V_4O_{10}$ microflowers.

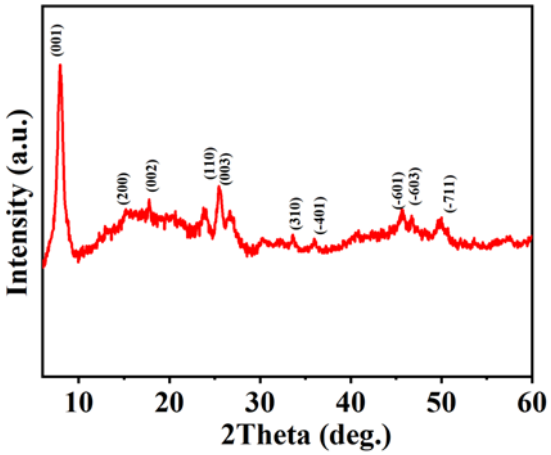

Figure S2. XRD patterns of precursor $NH_4V_4O_{10}$.

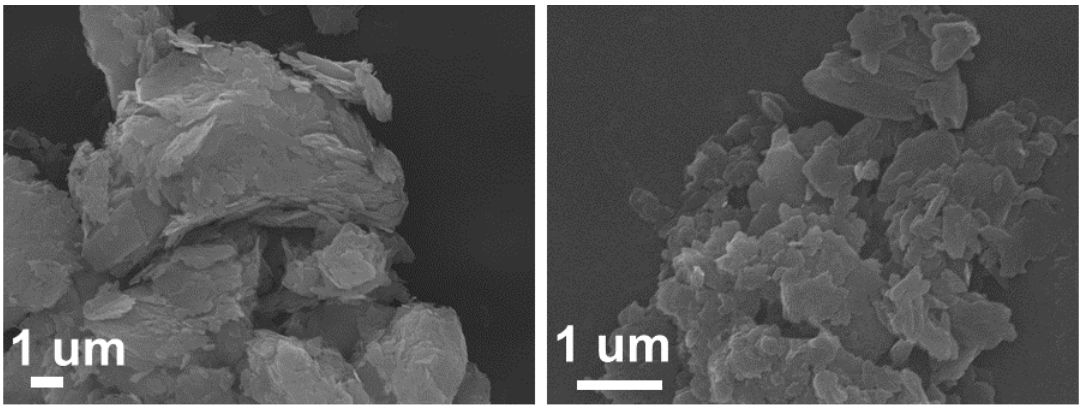

Figure S3. SEM images of the prepared V_6O_{13}.

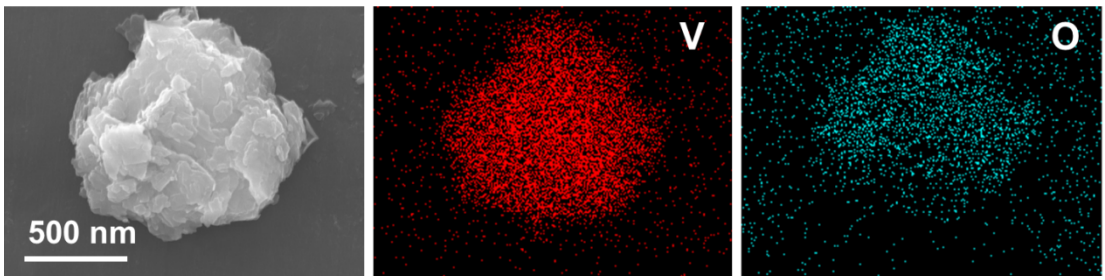

Figure S4. SEM-Mapping of the prepared V_6O_{13}.

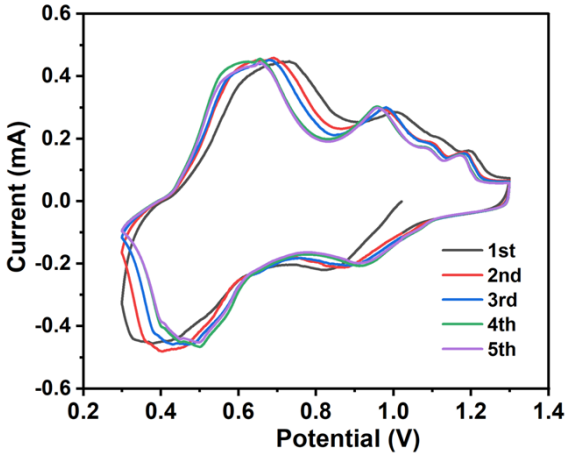

Figure S5. CV curves of the $NH_4V_4O_{10}$ microflowers at 0.1 mV s^{-1}.

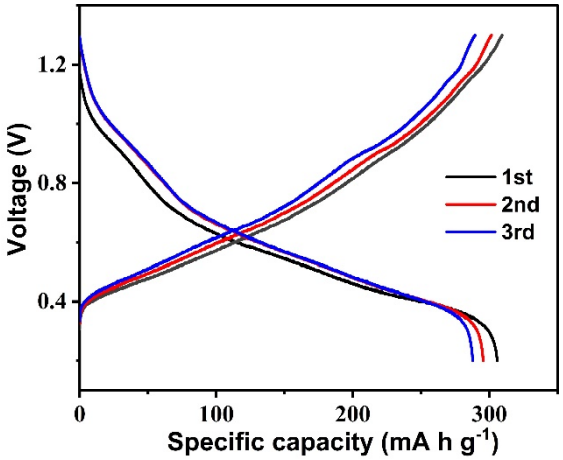

Figure S6. GCD curves of the Zn/$NH_4V_4O_{10}$ cell in the initial three cycles at the current density of 50 mA g^{-1}.

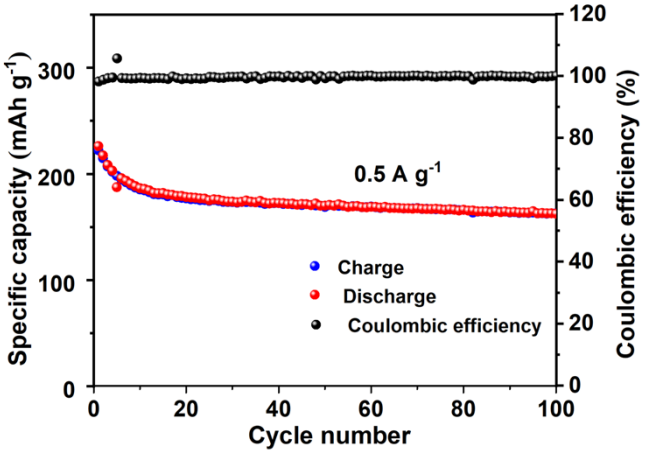

Figure S7. Cycling performance of $Zn/NH_4V_4O_{10}$ battery at 500 mA g^{-1}.

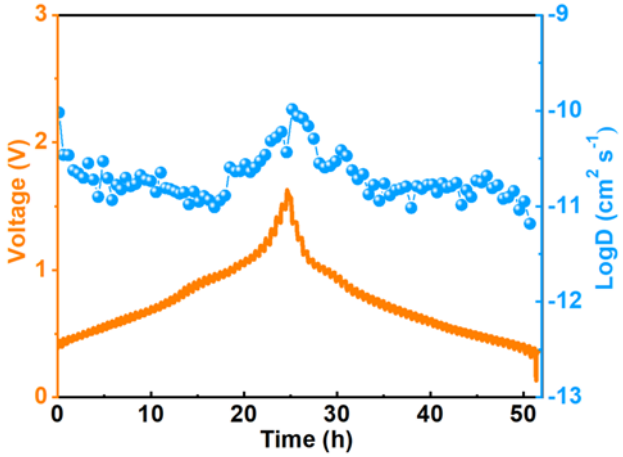

Figure S8. GITT curves and calculated Zn^{2+} diffusion coefficient of the V_6O_{13} cathode.

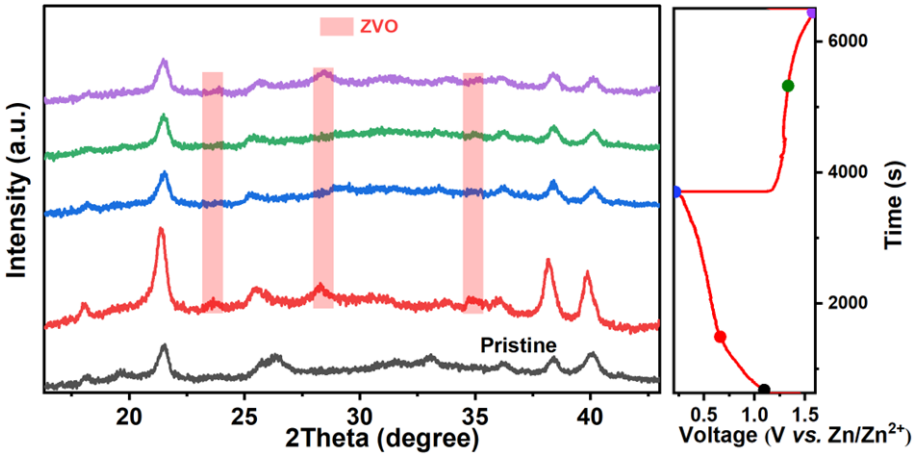

Figure S9. Ex-situ XRD patterns of prepared V_6O_{13} at the first cycle.

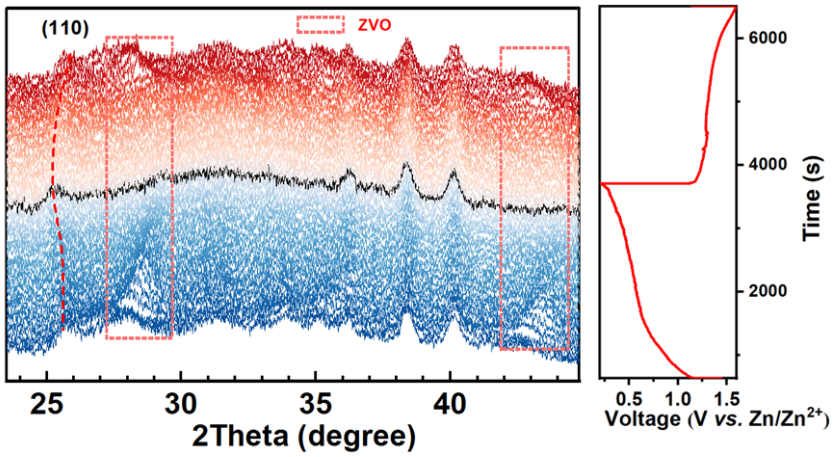

Figure S10. In-situ XRD patterns of the prepared V_6O_{13} at the second cycle.

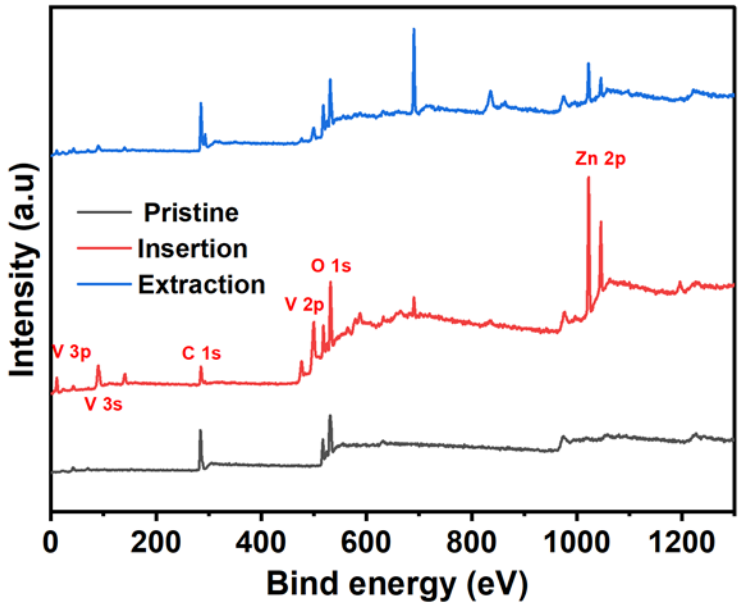

Figure S11. Ex-situ fully XPS spectra of prepared V_6O_{13} at the pristine, inserted and extracted states.

Supplementary Table

Table S1. Comparison of the electrochemical performance between this work and other V_6O_{13} cathode materials in AZIBs.

Materials	**Specific capacity (mA h g^{-1}/A g^{-1})**	**Cycleing performance (mA h g^{-1}/A g^{-1} /cycles)**	**Ref.**
V_6O_{13} nanosheets	425/0.05, 290/0.5	68/8/3000	**This work**
V_6O_{13}	220/0.1,142/1	112/1/3000	1
V_6O_{13}	360/0.2	230/4/2000	2

V_6O_{13}	350/0.1	206/10/3000	3
Tungsten-doped V_6O_{13}	325/0.2	225/3.2/1000	4
CO_2-incorporated V_6O_{13}	471/0.1	~80/2/4000	5
V_6O_{13} nanobelts on carbon cloth	290/0.375	227/9/1000	6
Oxygen-deficient V_6O_{13}	401/0.2	398/0.2/200	7
$V_6O_{13}\cdot nH_2O$	395/0.1	151/5/1000	8

Supplementary Note

Galvanostatic intermittent titration study

The Galvanostatic intermittent titration technique (GITT) was applied to determine the thermodynamic voltage-composition relationship, which corresponds to the equilibrium phase diagram of the system. The Zn^{2+} diffusion coefficients ($D_{Zn^{2+}}$) in V_6O_{13} were calculated from the GITT data. In the GITT, the transient voltage generated due to the application of a current pulse is monitored as a function of time. In our study, a galvanostatic pulse (charge or discharge) at 20 mA g^{-1} of 10 min is employed, followed by 30 min open circuit step to allow relaxation to equilibrium. The $D_{Zn^{2+}}$ value of the V_6O_{13} electrode (Figure. S5) was evaluated by the following equation:[9]

$$D^{\mathrm{GITT}} = \frac{4}{\pi\tau}\left(\frac{m_B V_M}{M_B S}\right)^2\left(\frac{\Delta E_S}{\Delta E_\tau}\right)^2 \quad (1)$$

where τ refers to constant current pulse time, m_B, V_M, M_B, and S are the mass, molar volume, molar mass of the cathode material, and electrode-electrolyte interface area, respectively. ΔE_S is voltage difference during a single-step experiment, and

ΔE_τ is the total change of cell voltage during a constant current pulse excluding the IR drop.

1. W. Wang, C. Yang, X. Chi, J. Liu, B. Wen and Y. Liu, *Energy Storage Mater.*, 2022, **53**, 774-782.
2. J. Shin, D. S. Choi, H. J. Lee, Y. Jung and J. W. Choi, *Adv. Energy Mater.*, 2019, **9**, 1900083.
3. L. Shan, J. Zhou, W. Zhang, C. Xia, S. Guo, X. Ma, G. Fang, X. Wu and S. Liang, *Energy Technol-GER*, 2019, **7**, 1900022.
4. J. Ding, J. Zhao, K. Zhao, S. Wang, S. Wu and S. Fang, *Small*, 2023, **19**, e2304130.
5. W. Shi, B. Yin, Y. Yang, M. B. Sullivan, J. Wang, Y. W. Zhang, Z. G. Yu, W. S. V. Lee and J. Xue, *ACS Nano*, 2021, **15**, 1273-1281.
6. M. Tamilselvan, T. V. M. Sreekanth, K. Yoo and J. Kim, *Appl. Surf. Sci.*, 2020, **529**, 147077.
7. M. Liao, J. Wang, L. Ye, H. Sun, Y. Wen, C. Wang, X. Sun, B. Wang and H. Peng, *Angew Chem. Int. Edit.*, 2020, **59**, 2273-2278.
8. J. Lai, H. Zhu, X. Zhu, H. Koritala and Y. Wang, *ACS Appl. Energy Mater.*, 2019, **2**, 1988-1996.
9. X. H. Rui, N. Ding, J. Liu, C. Li and C. H. Chen, *Electrochim. Acta*, 2010, **55**, 2384-2390.